Forcing of south-east African wet phases during the last 17,000 years

Enno Schefuß[1*], Holger Kuhlmann[1], Gesine Mollenhauer[1,2], Matthias Prange[1], Jürgen Pätzold[1]

[1]MARUM – Center for Marine Environmental Sciences and Faculty of Geosciences, University of Bremen, D-28359 Bremen, Germany

[2]Alfred Wegener Institute for Polar and Marine Research, D-27568 Bremerhaven, Germany

*email: schefuss@uni-bremen.de

Intense debate persists about the climatic mechanisms governing hydrological changes in tropical and subtropical southeast Africa since the last glacial maximum. In particular, the relative importance of atmospheric and oceanic processes is not firmly established[1-5]. Southward shifts of the Intertropical Convergence Zone (ITCZ) driven by high latitude climate changes have been suggested as a primary forcing[2,3], whereas other studies infer a predominant influence of Indian Ocean sea-surface temperatures (SSTs) on regional rainfall changes[4,5]. To address this question, a continuous record representing an integrated signal of regional climate variability is required, but has heretofore been missing. Here we show that remote atmospheric forcing by cold events in the northern high latitudes appears to be the main driver of southeast African hydro-climatology during rapid climate changes over the past 17,000 years. Our results are based on a reconstruction of precipitation and river discharge changes, as recorded in a marine sediment core off the mouth of the Zambezi River, near the southern boundary of the modern seasonal ITCZ migration. Phases of high precipitation and terrestrial discharge are detected for Heinrich Stadial 1 and the Younger Dryas, forced by southward ITCZ shifts, as well as

for the late Holocene, driven by high local summer insolation. Comparison to SST estimates indicates no primary control by Indian Ocean SST. Instead, regional precipitation changes responded directly to latitudinal shifts of the ITCZ and local insolation.

Climate changes reconstructed from Lake Malawi, the southernmost of the East African Great Lakes and located within the Zambezi catchment, point to arid conditions and strong northerly wind anomalies during Northern Hemisphere cold events such as the Younger Dryas (YD)[2,3]. It has been inferred that these periods represent southward shifts of the ITCZ[2,3,6]. Dry conditions during the YD and Heinrich Stadial 1 (HS1) in Lake Tanganyika, located closer to the equator in East Africa, were interpreted to have been caused by lowered Indian Ocean SST[4]. Recently, wide-spread drought conditions during HS1 in East Africa have similarly been suggested to be driven by cold conditions in the Indian Ocean[5]. Such interpretations are based on meteorological observations that modern rainfall in eastern and southern Africa is strongly related to high SST in the western and south-western Indian Ocean, respectively[7]. In contrast, Lake Chilwa located south-east of Lake Malawi, recorded high-stands, which appear to be solely associated with northern Hemisphere cold events[8]. Further westward in the interior of subtropical southern African, paleo-environmental information is sparse. Age dating of dunes in western Zambia and western Zimbabwe points to dry conditions at 18-17,000, 15-14,000, 11-8,000, and 6-4,000 years[9] before present (BP) implying that non-dune building periods around 16,000 and from 13-12,000 years BP roughly correspond to the wet periods found at Lake Chilwa[8]. Paleo-shorelines and other geomorphologic evidence from the Central Kalahari point to the existence of an extended lake system around the time of HS1 and around 8,500 years BP, with evidence for the existence of smaller lakes around the time of the YD[10]. It thus appears that the climatic history of subtropical southern

Africa is complex, and the importance of the various potential climatic forcing mechanisms remains unresolved.

To provide more insights into the climatic forcing of hydrology and land-ocean linkages in south-east Africa, we present a reconstruction of precipitation changes in the Zambezi catchment and its sedimentary discharge fluctuations in conjunction with SST estimates of the south-west Indian Ocean. The Zambezi catchment is located at the southern boundary of the present-day seasonal ITCZ migration and thus ideally suited to have recorded past changes in its southward extension. Under modern conditions, austral summer rainfall associated with the ITCZ extends to 15-20°S[6] (Fig. 1a,b). A low pressure cell forms over southern Africa during summer and attracts moisture from the tropical Atlantic by tropical westerly, and from the Indian Ocean by easterly air flow[6]. Atlantic moisture influences are restricted to the highlands south of the Congo basin, separated by the Congo Air Boundary from the majority of subtropical southern Africa receiving moisture from the Indian Ocean[11]. During austral winter a high pressure system over southern Africa leads to dry conditions, except in a small winter rainfall zone at its south-western tip[6]. The Zambezi River is the fourth-largest river in Africa originating in Zambia and flowing south-eastward to the Indian Ocean. The upper Zambezi is separated from its lower part by the Victoria Falls. After flowing through a series of gorges, the river enters a broad valley and spreads out over a large floodplain in its lower part. About 150 km from the coast, the catchment narrows where the river flows through the eastern Rift mountains. Maximum rainfall in the catchment during the peak of the southward ITCZ migration occurs in this area[12] (Fig. 1b), periodically causing extensive flooding[13]. The floodplain is dominated by papyrus swamps (dominated by *Cyperus papyrus*, a C_4 plant) with lower importance of reed swamps (*Phragmites* and *Typha*, C_3 plants)[14].

The C_4 plant dominance in the lower Zambezi floodplain is seen in the relative abundance of C_4 plants (Fig. 1c, d)[15]. Downstream from the Rift mountains, the Zambezi splits up into a flat and wide delta[13]. Woodlands, savannah and extensive mangrove forests (C_3 plants) vegetate the delta and coastal areas[14].

The 6.51 m long marine sediment core GeoB9307-3 (18°33.9'S, 37°22.8'E, 542 m water depth) was retrieved about 100 km off the Zambezi delta. The core location is in the zone of high deglacial-Holocene sedimentation of material discharged by the Zambezi River[16]. The chronology of the core is established by 19 ^{14}C AMS dates on mixed planktonic foraminifera (Tab. S1). Based on this chronology, it covers the last 17,000 years. Average time-resolution between the 125 samples is 130 years. We detect large increases in sedimentary terrestrial versus marine elemental ratios (Fig. 2b), in relative soil organic matter contributions[17] (Fig. 2c), and in sedimentary concentrations of terrestrial plant-derived long-chain *n*-alkanes (Fig. 2d) for the time periods of HS1 and the YD indicating enhanced terrestrial discharge by the Zambezi River. The elevated concentrations of *n*-alkanes indicate sustained vegetation cover during HS1 and the YD. Decreases of soil pH estimates during these intervals (see supplementary material) suggest higher rainfall as primary cause. For all these parameters, a slight increase is also detected for the late Holocene compared to the early Holocene. Comparison to records from Lake Malawi[2,3] suggests that the rainfall maximum associated with the ITCZ shifted southward of the Malawi basin during HS1 and the YD causing arid conditions at Lake Malawi while increasing rainfall in the lower Zambezi catchment. The stronger increases in these discharge-related parameters during the YD and HS1 compared to the late Holocene points to the influence of sea-level changes. Sea-level was reduced during the last deglaciation[18] resulting in a more proximal location of the Zambezi outflow to the core site. In order to investigate the continental hydrologic changes without influence of sea-level changes, we analysed the hydrogen isotopic composition of higher-plant derived lipid biomarkers. Hydrogen isotope compositions of the *n*-C_{31} alkane range from -136 to -164 ‰ VSMOW showing depleted values from 16,950 to 14,700 years BP, corresponding to the period of HS1, and from 12,800 to 11,350 years BP, representing the YD period (Fig. 2e). In the early Holocene most enriched values are found followed by a gradual decline towards the late Holocene interrupted by several short-term excursions to more enriched values. The *n*-C_{31} alkane derives from the protective wax coating of terrestrial higher plant leaves[19]. Its hydrogen isotope composition reflects changes in the isotopic composition of precipitation with potential enrichment due to evaporation from soils and evapo-transpiration from leaves[20], amplifying the recorded signal under arid conditions[21]. In monsoonal regions depleted isotopic composition of precipitation are indicative of rainfall amount changes[22]. These data suggest that changes in rainfall amount caused the discharge pulses detected for the YD and HS1.

Comparison of the δD values of the long-chain plant-waxes with their stable carbon isotope ($\delta^{13}C$) compositions reveals that sedimentary *n*-alkanes with depleted δD values show a stronger C_4 plant signal and vice versa (Fig. 2f). As C_4 plants are usually more drought-tolerant than C_3 plants[23], this correlation is unexpected. Although long-term vegetation changes are not ruled out (see supplementary material), the strong coherence of both isotopic signals, however, rather points to a shift in source area associated to the hydrologic changes as the primary cause for the observed relation. We infer that when maximum rainfall and flooding occurs in the floodplain, like under modern-day conditions, more C_4 plant-derived waxes are exported to the ocean, as reflected in the core-top isotopic signature (Fig. 1d, 2e).

Under more arid conditions, such as during the early Holocene, the export of C_4 plant-derived lipids from the floodplain was diminished and only low amounts of predominantly C_3 plant-derived waxes from near-coastal vegetation were exported. We thus deduce that the terrestrial signal in core GeoB9307-3 is predominantly derived from the lower Zambezi catchment dominated by changes in relative contributions from the floodplain. Aeolian transport of terrigenous material from subtropical southern Africa towards the south-west Indian Ocean is negligible due to the prevailing easterly winds[12].

Part of the signal seen in the δD record may thus derive from the changes in relative contributions from different vegetation types seen in the C_3/C_4 changes (e.g., ref 24). Although we cannot completely rule out this possible effect, the evidence provided by the other parameters (Fe/Ca ratio, Bit index, *n*-alkane concentrations, soil pH estimates) indicates that the depleted δD values during HS1, the YD and the late Holocene indeed reflect increased precipitation in the lower Zambezi floodplain.

The long-term trends in the δD and the $\delta^{13}C$ records correlate with mean summer insolation (Fig. 2g) over southern Africa[25]. Higher insolation intensifies atmospheric convection leading to higher rainfall over southern Africa[26]. For Heinrich events, modelling results indicate an increase of precipitation associated with isotopically depleted rainfall over southern Africa[27]. The magnitude of the modelled isotopic changes is consistent with our findings for HS1. A detailed comparison of the isotopic plant-wax changes with the oxygen isotope changes in the NGRIP ice core[28] (Fig. 3), which reflect northern high-latitude temperature changes, reveals a synchronous onset and end of the YD and a synchronous end of HS1. This synchronicity supports our conclusion that the plant waxes are not transported over long distances. As suggested by other studies[8-10], rainfall during HS1 and the YD likely also increased in the western parts of the Zambezi catchment. However, plant waxes derived from these more inland parts would carry a much more depleted δD signal due to increased moisture rainout during long-distance transport[29]. We thus infer that long-distance transport of plant waxes by the Zambezi River is of minor importance. Furthermore, the detected synchronicity of isotopic changes suggests a direct forcing of south-east African wet phases by Northern Hemisphere cold events and points to a large-scale atmospheric tele-connection(e.g., ref 30). Likely, persistent cold conditions in the Northern Hemisphere forced the ITCZ to a more southerly position during these events. The deviations in the amplitudes of isotopic changes of the ice core and the plant waxes during HS1 (Fig. 3) are likely explained by the modulation of rainfall intensity by local insolation.

In order to evaluate the effect of south-west Indian Ocean SST changes on continental hydrology, we compare the terrestrial records to a TEX_{86}-based SST record from GeoB9307-3 (Fig. 2g). The high BIT values in part of the record did not lead to a substantial bias in SST estimates (see supplementary material). The SST record shows warm conditions during the YD, however, does not indicate similarly warm conditions during HS1. Moreover, the timing of SST changes does not correspond to the observed hydrological changes. Therefore, we suggest that sufficiently warm conditions in the south-west Indian Ocean may have been an important pre-conditioning for southward movements of the ITCZ and the supply of moisture, but that rainfall changes in the Zambezi catchment over these time-scales were not primarily driven by these SSTs. We find no evidence for drought conditions in south-east Africa during HS1 driven by cold conditions in the Indian Ocean[5].

In summary, we conclude that rainfall and discharge changes in the Zambezi catchment result from a combination of local insolation and latitudinal ITCZ shifts with the latter being directly forced by high-latitude climate changes in the Northern Hemisphere. South-west Indian Ocean SST changes appear not to be the primary forcing of past hydrologic changes but may form an important pre-requisite.

Methods Summary

Element intensities were measured in 1 cm resolution using a XRF-I core scanner. The central sensor unit is equipped with a molybdenum X-ray source (3 – 50 keV), a Peltier-cooled PSI detector with a 125 µm beryllium window, and a multichannel analyzer with 20 eV spectral resolution. XRF data for this study were collected over a 1 cm^2 area using 30 seconds count time, 20 kV X-ray voltage and an X-ray current of 0.087 mA.

Sediments were extracted with a DIONEX Accelerated Solvent Extractor using dichloromethane:methanol (9:1; v/v). Saturated hydrocarbon fractions were obtained using silica column chromatography by elution with hexane and subsequent elution over $AgNO_3$-coated silica. Squalane was added before extraction as internal standard. Hydrogen isotope compositions of lipids were analysed on a Trace GC coupled via a pyrolysis reactor to a MAT 253 mass-spectrometer. Isotope values were measured against calibrated H_2 reference gas. δD values are reported in ‰ VSMOW. Further technical information is provided in the supplementary material. Compound-specific stable carbon isotope values were analysed on a Trace GC coupled via a combustion reactor to a MAT 252 mass-spectrometer. Isotope values were measured against calibrated CO_2 reference gas. $\delta^{13}C$ values are reported in ‰ VPDB. Further technical information is provided in the supplementary material. Polar fractions of the total lipid extracts eluted from silica columns with dichloromethane:methanol (1:1; v/v) were filtered through a 4-µm pore size PTFE filter and dissolved in hexane/isopropanol (99:1; v/v) prior to analysis by high performance liquid chromatography / atmospheric pressure chemical ionization – mass spectrometry (HPLC/APCI-MS). An Agilent 1200 series HPLC/APCI-MS system equipped with a Grace Prevail Cyano column (150 mm x 2.1 mm; 3 μm) was used, and separation was achieved in normal phase.

References

1 Clement, A. C. and Peterson, L. C., Mechanisms of abrupt climate change of the last glacial period. *Reviews of Geophysics* **46** (4), RG4002 (2008).

2 Johnson, T.C. et al., A high-resolution paleoclimate record spanning the past 25,000 years in southern east Africa. *Science* **296**, 113 (2002).

3 Castaneda, I. S., Werne, J. P., and Johnson, T. C., Wet and arid phases in the southeast African tropics since the Last Glacial Maximum. *Geology* **35** (9), 823 (2007).

4 Tierney, J. E. et al., Northern Hemisphere controls on tropical southeast African climate during the past 60,000 years. *Science* **322** (5899), 252 (2008).

5 Stager, C.J. , Ryves, D.B., Chase, B. M., and Pausata, F.S.R., Catastrophic drought in the Afro-Asian monsoon region during Heinrich Event 1. *Science* **331**, 1299 (2011).

6 Gasse, F. et al., Climatic patterns in equatorial and southern Africa from 30,000 to 10,000 years ago reconstructed from terrestrial and near-shore proxy data. *Quaternary Science Reviews* **27** (25-26), 2316 (2008).

7 Jury, M. R., Enfield, D. B., and Melice, J. L., Tropical monsoons around Africa: stability of El Nino-Southern Oscillation associations and links with continental climate. *Journal of Geophysical Research* **107** (C10) (2002); Ummenhofer, C. C., Sen Gupta, A., England, M. H., and Reason, C. J. C., Contributions of Indian Ocean Sea Surface Temperatures to Enhanced East African Rainfall. *Journal of Climate* **22** (4), 993 (2009).

8 Thomas, D. S. G. et al., Late Quaternary highstands at Lake Chilwa, Malawi: Frequency, timing and possible forcing mechanisms in the last 44 ka. *Quaternary Science Reviews* **28** (5-6), 526 (2009).

9 Thomas, D. S. G. and Shaw, P. A., Late Quaternary environmental change in central southern Africa: new data, synthesis, issues and prospects. *Quaternary Science Reviews* **21** (7), 783 (2002).

10 Burrough, S. L., Thomas, D. S. G., and Singarayer, J. S., Late Quaternary hydrological dynamics in the Middle Kalahari: Forcing and feedbacks. *Earth-Science Reviews* **96** (4), 313 (2009).

11 Gimeno, L. et al., On the origin of continental precipitation. *Geophysical Research Letters* **37**, L13804 (2010).

12 Nicholson, S.E., The nature of rainfall variability over Africa on time scales of decades to millennia. *Global and planetary change* **26**, 137 (2000).

13 Beilfuss, R. and dos Santos, D., *Patterns of Hydrological Change in the Zambezi Delta, Mozambique. Working Paper No. 2*. (International Crane Foundation, Sofala, Mozambique, 2001).

14 Beilfuss, R., Moore, D., Bento, C. , and Dutton, P., *Patterns of Vegetation Change in the Zambezi Delta, Mozambique. Working Paper No. 3*. (International Crane Foundation, Sofala, Mozambique, 2001).

15 Still, C. J. and Powell, R. L., in *Understanding movement, pattern, and process on Earth through isotope mapping*, edited by J.B. West, G.J. Bowen, T.E. Dawson, and K.P Tu (Springer, 2010).

[16] Schulz, H., Lückge, A., Emeis, K.-C., and Mackensen, A., Variability of Holocene to Late Pleistocene Zambezi riverine sedimentation at the upper continental slope off Mozambique, 15°–21°S. *Marine Geology* **286**, 21 (2011).
[17] Hopmans, E.C., Schefuß, E., Sinninghe Damsté, J.S., and Schouten, S., A novel proxy for terrestrial carbon input based on branched and isoprenoid tetraethers. *Earth and Planetary Science Letters* **224**, 107 (2004).
[18] Fairbanks, R.G., Sea level rise during the last deglaciation as recorded in Barbados corals. *Nature* **342**, 637 (1989).
[19] Eglinton, G. and Hamilton, R.J., Leaf epicuticular waxes. *Science* **156**, 1322 (1967).
[20] Sachse, D., Radke, J., and Gleixner, G., dD values of individual n-alkanes from terrestrial plants along a climatic gradient - Implications for the sedimentary biomarker record. *Organic Geochemistry* **37**, 469 (2006).
[21] Schefuß, E., Schouten, . S., and Schneider, R.R., Climatic controls of Central African hydrology during the last 20,000 years. *Nature* **437**, 1003 (2005).
[22] Risi, C., Bony, S., and Vimeux, F., Influence of convective processes on the isotopic composition (delta(18)O and delta D) of precipitation and water vapor in the tropics: 2. Physical interpretation of the amount effect. *J. Geophys. Res.-Atmos.* **113** (D19) (2008).
[23] Ehleringer, J.R. and Cerling, T.E., in *Encyclopedia of Global Environmental Change*, edited by T. Munn (John Wiley & Sons, Ltd, Chichester, 2002), Vol. 2, pp. 186.
[24] Hou, J. Z., D'Andrea, W. J., MacDonald, D., and Huang, Y. S., Hydrogen isotopic variability in leaf waxes among terrestrial and aquatic plants around Blood Pond, Massachusetts (USA). *Organic Geochemistry* **38** (6), 977 (2007).
[25] Laskar, J. et al., A long-term numerical solution for the insolation quantities of the Earth. *Astronomy & Astrophysics* **428** (1), 261 (2004).
[26] Partridge, T.C. et al., Orbital forcing of climate over South Africa: a 200,000 year rainfall record from the Pretoria Saltpan. *Quaternary Science Reviews* **16**, 1125 (1997).
[27] Lewis, S. C., LeGrande, A. N., Kelley, M., and Schmidt, G. A., Water vapour source impacts on oxygen isotope variability in tropical precipitation during Heinrich events. *Climate of the Past* **6** (3), 325 (2010).
[28] Andersen, K. K. et al., High-resolution record of Northern Hemisphere climate extending into the last interglacial period. *Nature* **431** (7005), 147 (2004).
[29] Frankenberg, C. et al., Dynamic Processes Governing Lower-Tropospheric HDO/H(2)O Ratios as Observed from Space and Ground. *Science* **325** (5946), 1374 (2009).
[30] Broccoli, A.J., Dahl, K.A., and Stouffer, R.J., Response of the ITCZ to Northern Hemisphere cooling. *Geophysical Research Letters* **33**, doi:10.1029/2005GL024546 (2006).

Acknowledgements

This work was supported by the DFG Research Center/Cluster of Excellence `The Ocean in the Earth System' and DFG grant Sche903/8. Laboratory assistance was provided by Katharina Siedenberg, Monika Segl, Wolfgang Bevern, Birgit Meyer-Schack and Ralph Kreutz. We thank Ralph Schneider for logistical support and Syee

Weldeab for sample preparation for radiocarbon analyses. Comments by Yongsong Huang, James Russell and an anonymous reviewer greatly improved the manuscript.

Author contributions

Experimental work was carried out by E.S., H.K., G.M. and J.P. Data analysis and interpretation were carried out by E.S., H.K., G.M., M.P. and J.P.

Additional information

The authors declare no competing financial interests. Supplementary information accompanies this paper on www.nature.com/nature. Reprints and permissions information is available online at http://npg.nature.com/reprintsandpermissions. Data are stored in the Pangaea database (www.pangaea.de).

Correspondence and requests for materials should be addressed to E.S.

Figure captions

Figure 1: Modern atmospheric circulation over southern Africa during southern Hemisphere summer, summer rainfall and vegetation types. a, Schematic representation of the atmospheric circulation over southern Africa during austral summer (December, January, February - DJF) with approximate position of the ITCZ and the Congo Air Boundary (CAB). Indicated are: the main course of the Zambezi River (blue), the Zambezi catchment (grey) and the location of GeoB9307-3 (red star). Red dots indicate locations of other records discussed in the text: 1) Lake Malawi[2], 2) Lake Tanganyika[4], 3) Lake Chilwa[8], 4) dunes in Zambia and Zimbabwe[9], and 5) paleo-shorelines in the Kalahari[10]. **b**, Austral summer (DJF) rainfall (cm month^{-1}) for the period 1950–1999 (University of Delaware data set; http://climate.geog.udel.edu/~climate/). Outline of the Zambezi catchment in white and main course of the Zambezi River in blue. **c**, Modern-day vegetation type distribution[15], shown as percentage of C_4 plants. White areas are either >95 % C_4 or not vegetated. Zambezi catchment and Zambezi River as in **b**. Black box indicates the area shown in **d**. **d**, Map of the relative C_4 plant abundance[15] in the lower Zambezi catchment. White areas are not vegetated. White box indicates the location of the lower Zambezi floodplain.

Figure 2: Records of environmental variability in southeastern Africa over the last 17,000 years. a, oxygen isotope changes in NGRIP ice core[28] mainly reflecting northern high-latitude temperature changes. **b**, Fe/Ca ratio indicating terrestrial versus marine elemental contributions to sediments of GeoB9307-3. **c**, BIT index of GeoB9307-3 reflecting changes in relative soil organic matter contribution. **d**,

concentrations of long-chain, odd-numbered *n*-alkanes (*n*-C_{25} – *n*-C_{35}) in the sediments of GeoB9307-3 (in ng/g). **e**, hydrogen isotope compositions of *n*-C_{31} alkanes in GeoB9307-3 reflecting rainfall changes in the Zambezi catchment. Error bars based on replicate analyses shown in Fig. S1. **f**, stable carbon isotope compositions of *n*-C_{31} alkanes in GeoB9307-3 indicating relative contribution changes from the lower Zambezi floodplain. Error bars based on replicate analyses shown in Fig. S2. **g**, Long-term insolation changes over southern Africa (20°S) during Southern Hemisphere summer (DJF)[25]. **h**, TEX_{86}-derived SST record from GeoB9307-3 reflecting ocean temperature changes in the south-west Indian Ocean. BP = before present. Grey bars indicate intervals of Heinrich Stadial 1 (HS1) and the Younger Dryas (YD). Black triangles indicate ^{14}C AMS ages.

Figure 3: Detailed comparison of Greenland climate changes with hydrological variations in the Zambezi catchment during the last deglaciation. Greenland temperature changes (blue) from the NGRIP ice core[28] compared to hydrogen isotope changes of the *n*-C_{31} alkane in sediments of GeoB9307-3 reflecting rainfall changes in the Zambezi catchment (black, note inverted scale). Short-term deviations in amplitudes are likely due to modulation of rainfall intensity by local insolation (Fig. 2g). BP = before present. Grey bars indicate intervals of Heinrich Stadial 1 (HS1) and the Younger Dryas (YD). Black triangles indicate ^{14}C AMS ages. Error bars based on replicate analyses shown in Fig. S1.

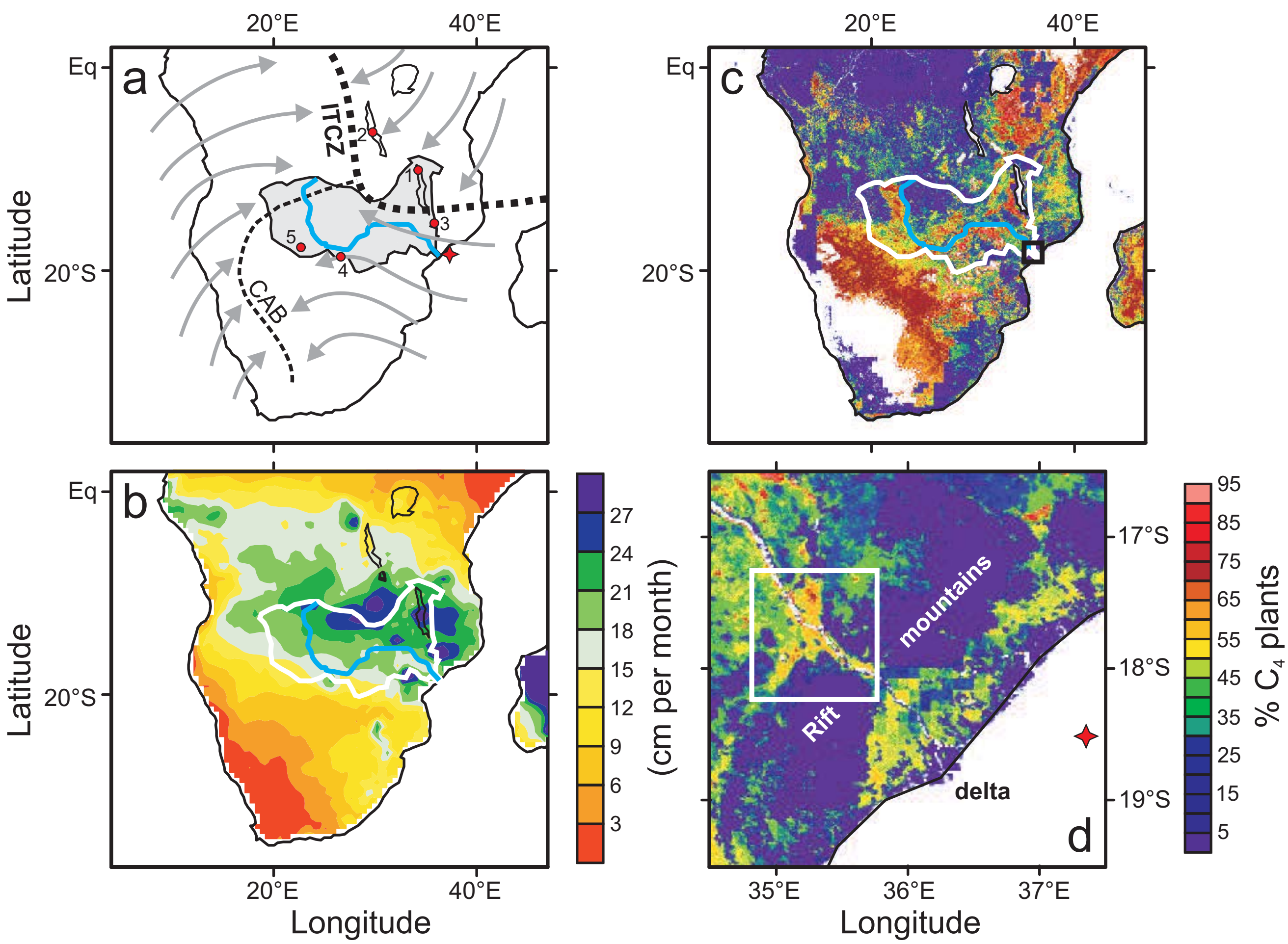

a
b
c
d
Eq
20°S
20°E
40°E
ITCZ
CAB
1
2
3
4
5
Latitude
Longitude
27
24
21
18
15
12
9
6
3
(cm per month)
17°S
18°S
19°S
35°E
36°E
37°E
mountains
Rift
delta
95
85
75
65
55
45
35
25
15
5
% C_4 plants

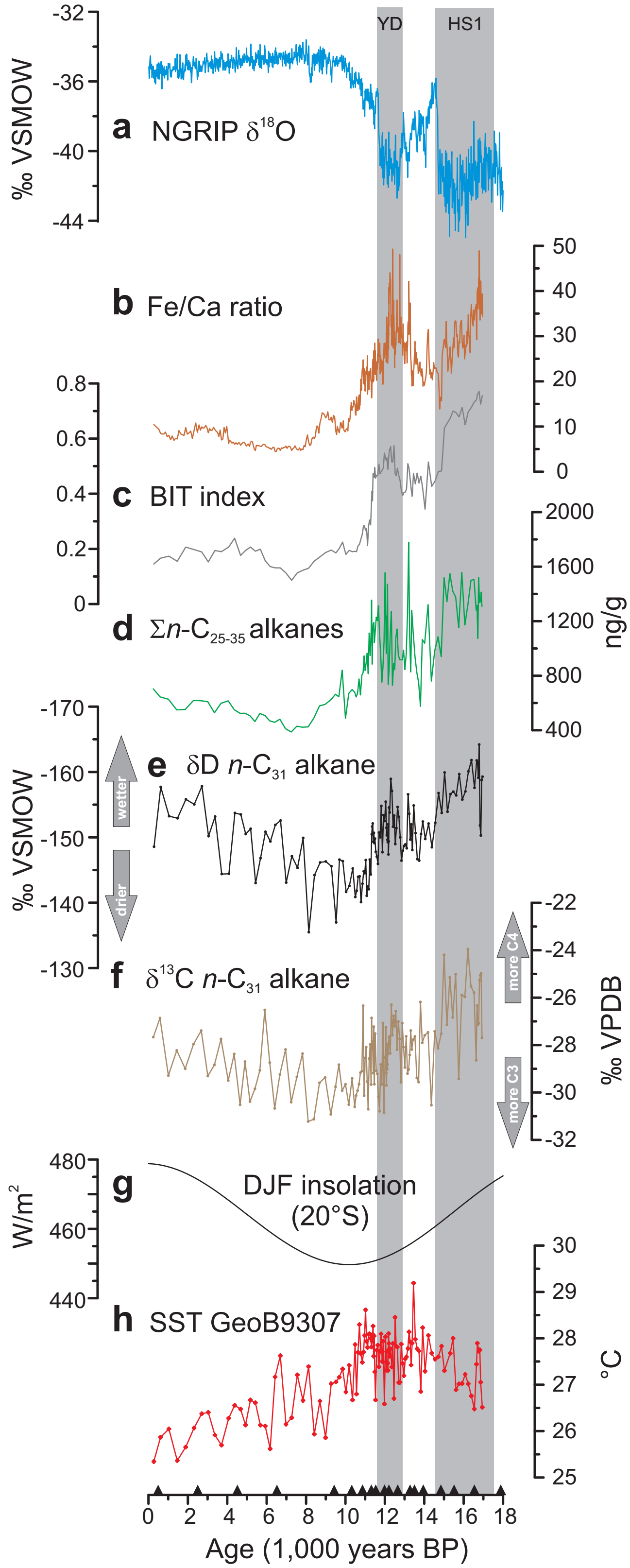
YD
HS1
a NGRIP δ18O
‰ VSMOW
-32
-36
-40
-44
b Fe/Ca ratio
50
40
30
20
10
0
c BIT index
0.8
0.6
0.4
0.2
0
d Σn-C25-35 alkanes
ng/g
2000
1600
1200
800
400
e δD n-C31 alkane
‰ VSMOW
-170
-160
-150
-140
-130
wetter
drier
f δ13C n-C31 alkane
‰ VPDB
-22
-24
-26
-28
-30
-32
more C4
more C3
g DJF insolation (20°S)
W/m2
480
460
440
h SST GeoB9307
°C
30
29
28
27
26
25
0 2 4 6 8 10 12 14 16 18
Age (1,000 years BP)

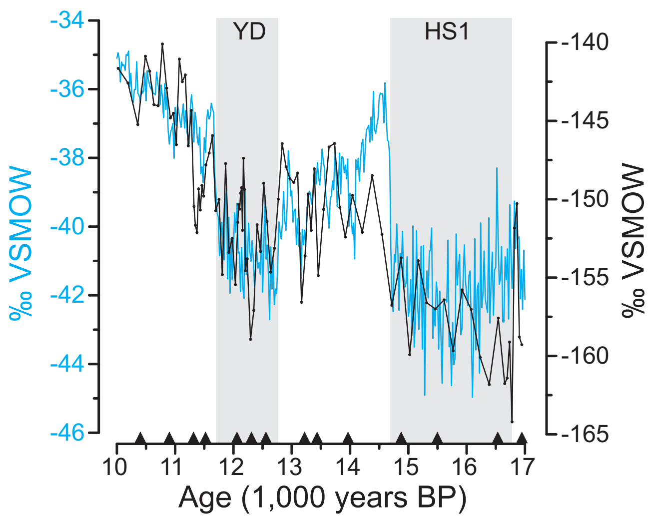

YD
HS1
-34
-36
-38
-40
-42
-44
-46
‰ VSMOW
-140
-145
-150
-155
-160
-165
‰ VSMOW
10
11
12
13
14
15
16
17
Age (1,000 years BP)